Scientia Iranica C (2023) 30(6), 2029–2042

Sharif University of Technology
Scientia Iranica
Transactions C: Chemistry and Chemical Engineering
http://scientiairanica.sharif.edu

Synthesis of a new porous Graphene Oxide Framework (GOF) for high-performance ultrasonic-assisted removal of cadmium and lead ions from aqueous solution

A. Shekarizadeh[a], R. Azadi[a,*], and R. Mirzajani[a,b]

a. *Department of Chemistry, Faculty of Science, Shahid Chamran University of Ahvaz, Ahvaz 61357-43169, Iran.*
b. *Drilling Center of Excellence and Research Center, Shahid Chamran University of Ahvaz, Iran.*

Received 28 June 2022; received in revised form 26 November 2022; accepted 2 May 2023

KEYWORDS
Porous graphene oxide framework;
Adsorption;
Sonication;
Removal;
Heavy metal ions;
Water.

Abstract. A novel chelating adsorbent was successfully synthesized by cross-linking of 4, 4′, 4″-*s*-triazine-1, 3, 5-triyltri-*p*-aminobenzoic acid as a linker with nanosheets of graphene oxide to provide a 3-dimensional framework. Therefore, the adsorption process of Cd^{+2} and Pb^{+2} on the adsorbent was investigated by employing an ultrasonic bath. The optimum condition containing the small amount of adsorbent (10 mg) for both metals at pH=8 for Cd^{+2} and pH=5 for Pb^{+2}, and a short time of two minutes caused gaining an absorption capacity at a high level. The presence of nitrogen-functionalized groups in the porous Graphene Oxide Framework (GOF) contributed to the absorption of lead and cadmium ions. The kinetic models of pseudo-first-order and pseudo-second-order were used to define the kinetic process. The experimental adsorption datum was properly suited to the kinetic model of the pseudo-second-order ($R^2 = 0.990$). It indicated that adsorbing ions of heavy metals onto GOF happens through a chemical process, and adsorption isotherms of Cd^{+2} and Pb^{+2} ions were in high-grade accordance with the Longmuir model. Eventually, because of the rapid adsorption kinetics, high removal capacity, perfect stability, and being reusable, this GOF can be used as a remediation adsorbent with high-performing heavy metals removal from aqueous solutions.

1. Introduction

Removing heavy metals from the environment is a significant subject, and developing new methods and adsorbents to achieve excellent removal efficiencies is much regarded [1,2]. The term "heavy metal" is utilized for any metallic element with high density (more than 5 grams per cubic centimeter) (e.g., copper, mercury, cadmium, lead, and arsenic) [3]. Accumulating such heavy metals in the human body can lead to cancer. Consequently, new technologies are needed to eliminate these toxic ions from pollution and wastewater. Therefore, to extract heavy metal ions from the aquatic environment, different scientific methods were developed, including electrodialysis, reverse osmosis, coagulation, ion-exchange, adsorption, chemical precipitation, flotation, filtration, irradiation, and membrane filtration [4–6]. Among these processes, adsorption is very common, and due to high efficiency, low cost, design simplicity, and selectivity, it is considered a promising strategy for extracting heavy metals from wastewater. In this context, to remove toxic ions, many substances have been widely adopted, including meso-

*. *Corresponding author. Tel.: +98-61-33331042; Fax: +98-61-33331041*
E-mail addresses: arzshekari@yahoo.com (A. Shekarizadeh); razadi@scu.ac.ir (R. Azadi); rmirzajani@scu.ac.ir (R. Mirzajani)

doi: 10.24200/sci.2023.60682.6933

porous zeolites [7], clay [8,9], carbon [10], polymers [11], Metal-Organic Frameworks (MOF) [12,13], and Covalent Organic Frameworks (COF) [14,15]. Nevertheless, most substances mentioned above have defects such as low sorption capacity, high cost, slow capture kinetics, use of toxic raw materials, and poor selectivity, reducing the perspective of practical application on an industrial scale [16,17]. Consequently, to remove heavy metals from the environment and polluted water, novel types of eco-friendly and stable adsorbents must be developed with an adsorption capacity at high levels. Designing an adsorbent with many convenient chelating sites with high affinity, high capacity, and rapid uptake of the pollutants is a crucial challenge in environmental remediation. In recent years, the use of graphene oxide-based nanomaterials and their three-dimensional (3D) configurations as new carbon-based adsorbents have superior adsorption properties toward toxic metal ions [10]. The graphene oxide's different functional groups, including epoxy, carboxyl, and hydroxyl, can bind covalently with the chelating linkers. These linkers, which strongly tend to coordinate with the metal ions, enhance the sorption capacity of the nanocomposites. For example, linkers with functional groups containing nitrogen display a mighty capability to coordinate with the ions of heavy metals [18–23]. Graphene Oxide Frameworks (GOFs) play their role in creating excellent adsorbents since they have proper mesopore constructions that can exhibit the right combination of properties to act as scaffolding to decorate coordination sites, in other words, 4, 4′, 4″-*s*-triazine-1, 3, 5-triyltri-*p*-aminobenzoic acid (H3TATAB) is an organic compound that has three nitrogen atoms in a triazine ring and three amine groups which be amongst the most efficient chelating functional groups towards heavy metal ions, especially Cd^{+2} and Pb^{+2} [24–27]. Therefore, TATAB was chosen as a cross-linker for the covalent modification of GO nanosheets to form a three-dimensional GOF as an exceptionally adsorbent to remove heavy metal ions from polluted water.

2. Experimental section

2.1. Materials and instrumentation

4-aminobenzoic acid, cyanuric chloride, sulfuric acid (H_2SO_4), hydrogen peroxide (H_2O_2), potassium permanganate ($KMnO_4$), and Graphite powder were bought from Merck chemical company (Kenilworth, NJ 07033, USA). Double-distilled water was used throughout the tests. The typical solutions of lead and cadmium were ready by dissolving suitable volumes of $Pb(NO_3)_2$ (Merck, Darmstadt, Germany) and $Cd(NO_3)_2.4H_2O$ (Sigma-Aldrich, USA) in deionized water.

A GBC Flame Atomic Absorption Spectrometer (FAAS) model Avanta (Australia) tailored with lead and cadmium hollow cathode lamps was employed for the examination. The contributory settings designated for lead and cadmium were 5.0 and 3.0 mA lamp current, 1.0 and 0.5 nm bandwidth of the slit, and 217 and 228.3 nm wavelength. An ultrasonic bath (Heidolph, Germany) at 60 Hz frequency was used for the ultrasound-assisted adsorption procedure. A Labtron vortex model ls-100 (Iran) was applied for rapid shaking. A Metrohm 827 pH meter (Switzerland) was used for pH measurements. The X-Ray powder Diffraction (XRD) patterns were recorded at 21°C with a PANalytical X′Pert Pro MPD instrument (Netherlands) by Cu-Kα radiation at 40 kV and 40 mA in the limited area of $2\theta = 5° - 80°$ with a stage size of 0.02. In the transition method, the Fourier Transform Infrared (FT-IR) spectra were recorded in the limited area of 4000 to 400 cm^{-1} by PerkinElmer (Spectrum Two, USA) spectrometer. Barrett-Joyner-Halenda (BJH) model and Brunauer-Emmett-Teller (BET) method accounted for the pore size distribution and particular surface area. Thermogravimetric analysis (TGA) of compounds was calculated with the STA-1500 calorimeter (STA 1500, Rheometric Scientific, USA). Synthesis of GO Energy Dispersive X-Ray (EDX) was recorded with a Mira 3-XMU instrument (USA).

GO was prepared from graphite through a modified Hummers method [28].

2.2. Synthesis of perhydroxylated Graphene Oxide (GOH)

GO (1.0 g) was dispersed in 30 mL deionized water in a dried 50 mL flask for 10 min, and then 1.0 g NaOH was added to the GO dispersed solution and stirred for 1 h at room temperature. In the following, the mixture temperature was increased to 90°C and was agitated for 24 h. After cooling the mixture to room temperature, the solution was acidified with 5% hydrochloric acid to pH=7. By centrifuging at 7000 rpm, the product was separated and washed with distilled water, and dried.

2.3. Synthesis of 4, 4′, 4″-s-triazine-1, 3, 5-triyltri-p-aminobenzoic acid (H3TATAB)

At first, a solution containing 4-aminobenzoic acid (1.8 g, 13.2 mmol), water 20 mL, and 3 mL of sodium hydroxide 5 M was prepared and then charged with sodium bicarbonate (0.9 g, 11 mmol). Then, a solution containing (0.6 g, 3.3 mmol) of cyanuric chloride and 1, 4- dioxane (5 mL) was gradually mixed. The blend was agitated at room temperature for 10 minutes, then for one night at 110°C under reflux conditions. To continue, after being balanced the mixture temperature in the room environment, 20% hydrochloric acid was added to bring the pH of the mixture to 3. After

centrifuging the suspension, the solids were removed with water. The accumulated bright yellow solid was dried in an oven to yield pure H3TATAB (1.8 g, 80%) [29].

2.4. Synthesis of 4, 4′, 4″-s-triazine-1, 3, 5-triyltri-p-aminobenzoyl chloride

A mixture of H3TATAB (0.48 g, 1 mmol) and $SOCl_2$ (10 mL) was refluxed at 70°C for 24 h. After vacuum distillation of $SOCl_2$, 4, 4′, 4″ − *s*-triazine-1, 3, 5-triyltri-*p*-aminobenzoyl chloride (0.44 g, 92%) was obtained.

2.5. Synthesis of GOF

The GOF was synthesized by the reaction of Graphene Oxide Hydrogel (GOH) with 4, 4′, 4″-*s*-triazine-1, 3, 5-triyltri-*p*-aminobenzoyl chloride. The GOH in the amount of 0.1 g was dissolved in 30 mL of dry dimethylformamide (DMF) and was exposed to ultrasonic waves for 30 minutes. Next, 4, 4′, 4″-*s*-triazine-1, 3, 5-triyltri-*p*-aminobenzoyl chloride (0.1 g, 0.2 mmol) was added to 20 mL of dry DMF, stirred, and slowly added to GOH suspension. Subsequently, the mixture was stirred for 24 h at 100°C. Finally, the mixture was kept under static conditions for 24 h at 80°C. The obtained solid was filtered and washed with THF and deionized water numerous times. Then, the product was dried in an oven, and GOF (0.17 g) was obtained.

2.6. Removal procedure

To study the effect of physicochemical factors, the batch equilibrium method was applied for the adsorption experiments. The effect of variables including initial pH of sample solutions (3–9), contact time (0.3–10 min), adsorbent dosage (5–15 mg), and the initial concentration of analyses (10–400 μg L^{-1}) on the adsorption efficiency of Cd^{+2} and Pb^{+2} using GOF was individually investigated. The stock standard solution (1000 μg L^{-1}) of Cd^{+2} and Pb^{+2} was prepared by dissolving a suitable value of $Cd(NO_3)_2$ and $Pb(NO_3)_2$ salts in 100 mL deionized water. The required concentration solution for the experiments was then prepared by diluting the stock standard solution. Initially, the Cd^{+2} and Pb^{+2} solutions were prepared at a concentration of 10 mg L^{-1}, and then 15 mL of each solution was transferred to a separate sample vessel. Next, the pH values of the sample were adjusted by adding a small amount of NaOH or HCl solutions (0.1 mol L^{-1}). Then, 10 mg of GOF as adsorbent was added to each sample and sonicated for 5 min. Afterward, the adsorbent was immediately removed from the solution and sampled for AAS. For equilibrium studies, 15 mL of different concentrations of metal ions were added to the sample containing 10 mg of adsorbent. Thereafter, the initial and residual concentrations of each metal ion were determined. It is noteworthy that we examined the same steps for cadmium and lead separately. The removal percentage ($R(\%)$) of metal ions was then calculated by the following equation:

$$R\ (\%) = \frac{C_i - C_e}{C_i} \times 100, \tag{1}$$

where C_i and C_e are the initial and equilibrium heavy metal concentrations (mg L^{-1}), respectively. The amount of the adsorbed metal ions at equilibrium q_e (mg g^{-1}) was then obtained by Eq. (2) as below:

$$q_e = \frac{(C_i - C_e)\, V}{m}, \tag{2}$$

where, V (L) is the volume of the solution, and m (g) is the weight of the adsorbent.

3. Results and discussion

Continuing our research on synthesizing a novel GOF as a catalyst [30], we present the synthesis of a new GOF and its application for the removal of cadmium and lead ions from an aqueous solution. The synthesis of GOF is illustrated in Scheme 1.

Graphene oxide platelets contain functional groups with oxygen, including epoxy and hydroxyl groups on the basal planes that are reactive chemically. At first, the reaction of graphene oxide with sodium hydroxide was performed to increase the hydroxyl group on graphene oxide for the reaction with the linker (Scheme 1(a)). The epoxy groups of graphene oxide can be simply improved over ring-opening reactions, including the nucleophilic attack at the α-carbon using the hydroxide anion. In the second step, 4, 4′, 4″-*s*-triazine-1, 3, 5-triyltri-*p*-aminobenzoic acid (H3TATAB) precursor was prepared through the reaction of 4-aminobenzoic acid with cyanuric chloride in the presence of a base. Then, produced H3TATAB is first converted to 4, 4′, 4″-*s*-triazine-1, 3, 5-triyltri-*p*-aminobenzoyl chloride using $SOCl_2$ and then reacted with GOH to synthesize GOF.

To study the chemical structure and morphology of GO and GOF, different analyses of FT-IR, EDX, XRD, TGA, and BET were carried out.

3.1. Characterization of GOF

The spectra of FT-IR for GOH, H3TATAB, and GOF have been presented in Figure 1. The vibrational bands related to O-H stretching at 3300 to 3500 cm^{-1}, the stretching vibration of C=O at 1720 cm^{-1}, the stretching vibration of C=C at 1618 cm^{-1}, and C-O and C-OH at 1080 to 1200 cm^{-1} were detected in the IR spectra of GOH. In IR spectra of H3TATAB, the stretching vibration of C-N at 1312 cm^{-1}, N-H bending vibration at 1498 cm^{-1}, N-H out-of-plane bending vibration at 795 cm^{-1}, the vibrational bands related to C=C, C=N at 1498–1602 cm^{-1}, the stretching vibration of C=O at 1700 cm^{-1} and the stretching vibration of N-H (secondary amine) at 3412 cm^{-1} were

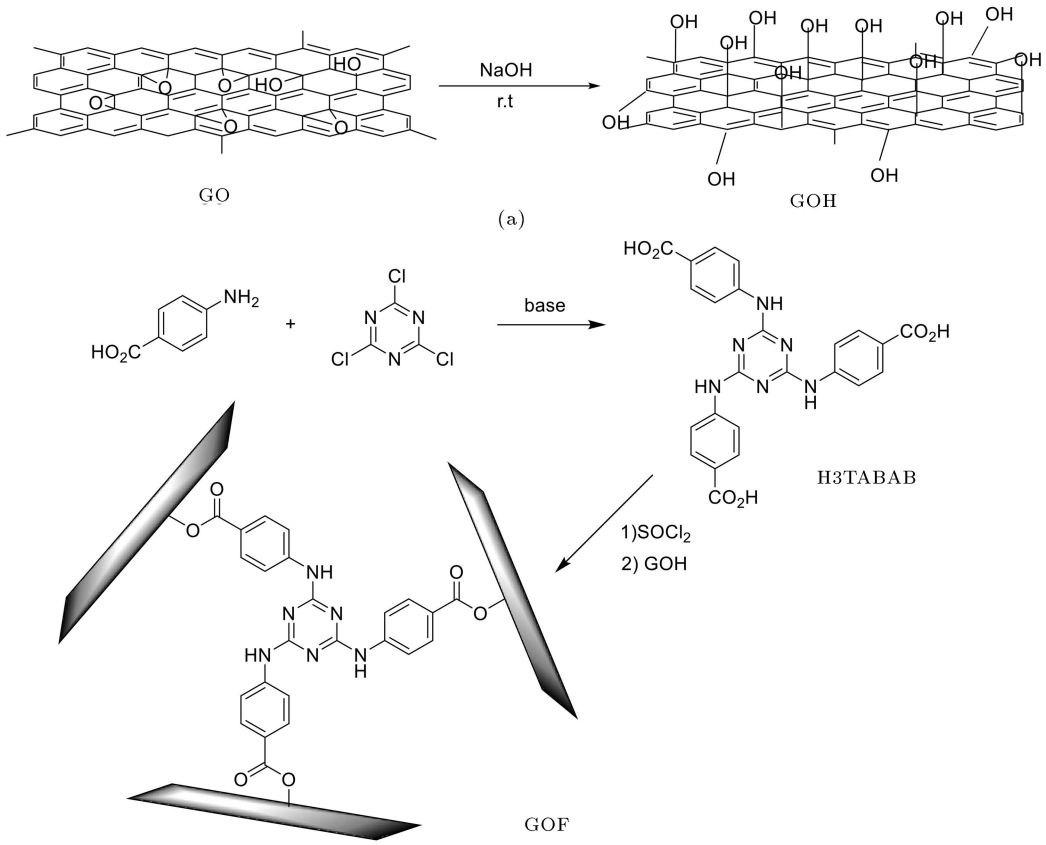

Scheme 1. Synthesis of graphene oxide framework.

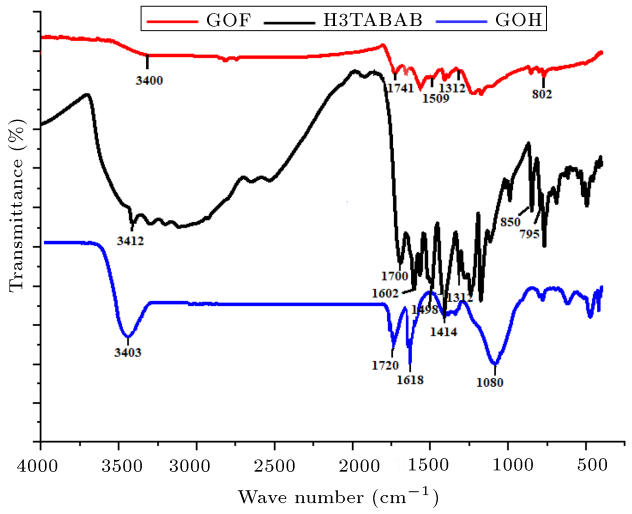

Figure 1. Fourier-transform infrared spectra of GOH, H3TATAB, and GOF.

detected. When the GOH cross-linked with H3TATAB, a novel adsorption band emerged at 1741 cm^{-1} and was attributed to stretching vibration relating to C=O of ester groups. Similarly, the absorption band of C-N at 1250–1350 cm^{-1}, N-H bending vibration at about 1509 cm^{-1}, N-H out-of-plane bending vibration at 802 cm^{-1}, and the C=O related to the ester group approved the linkage of H3TATAB to sheets of GO via esterification and fabrication of GOF.

Table 1. The elements quantity of GOF observed by EDS analysis.

C	N	O
59.82	21.41	18.77

In order to confirm the preparation of GOF with the mentioned linker and prove the presence of compositional elements, EDX analysis was examined (Figure 2). The existence of N atoms in the synthesized composite is related to the formation of GOF. The quantity of elements observed by EDS analysis is shown in Table 1.

The XRD analysis is usually employed to examine the substances' crystalline construction. Figure 3 illustrates the XRD patterns related to GOF and GO. The XRD pattern related to GO has displayed an amorphous nature with three peaks at $2\theta = 12°$, 26.50°, and 42.19°. Nevertheless, the diffraction peak of GO vanished in the XRD pattern related to GOF nanocomposite. It was displayed that the GO had a great exfoliation and scattering in the produced GOF. Moreover, in the XRD pattern related

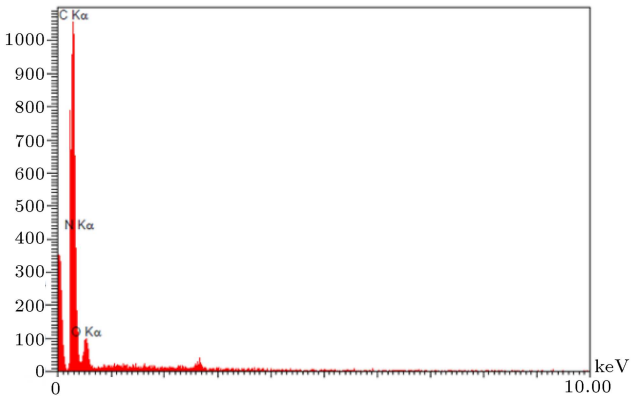

Figure 2. Energy-dispersive X-ray spectroscopy analysis of GOF.

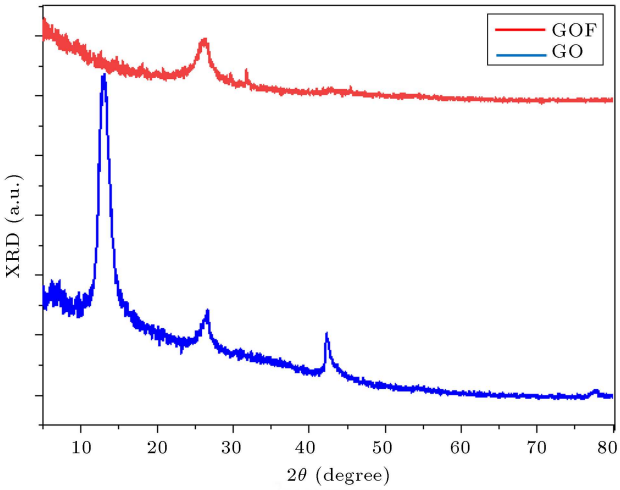

Figure 3. X-ray diffraction pattern of GO and GOF.

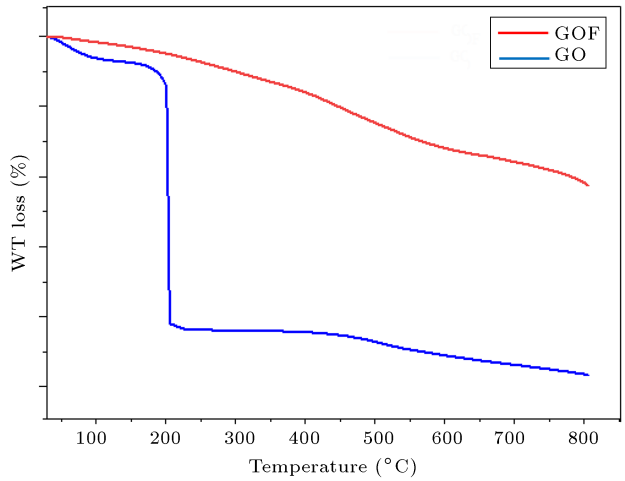

Figure 4. TGA curve of GO and GOF.

to GOF,only one broad peak at 26.60° indicated its amorphous nature and can be indexed to the reflection of graphene [31].

TGA was used to estimate the thermal stability related to GOF nanocomposite. The TGA curves of GO and GOF have been displayed in Figure 4. The initial weight loss for GO at 110°C was due to the adsorbed water's evaporation, and the maximum weight loss temperature from 190 to 210°C was assigned to the loss of functional groups of labile oxygen at the GO surface [32,33]. The sequential weight loss between 210–800°C can be attributed to the more stable phenol groups and the pyrolyzing of the carbon skeleton in the GO construction [34]. The TGA curve of GOF showed the thermal stability of the nanocomposite greater than that of GO. The TGA results also confirmed that the GOF has successfully formed.

The N_2 adsorption-desorption isotherms and pore size distribution have evaluated the porosity of GOF (Figure 5). The BET model was applied to account for the surface area of GO, which was 7.87 m^2 g^{-1}, while GOF's surface area was increased up to 14 m^2 g^{-1}. The BJH model calculated the average pore diameter, which led to about 19 nm (more details are in Table 2). N_2 adsorption-desorption isotherms of GOF are similar to type IV, which shows a distinct H3 hysteresis loop, denoting the GOF's mesoporous nature. These isotherms characterize the porous substances, and nitrogen molecules have condensed in the tiny capillary mesopores of the adsorbent [35,36]. This observation indicated the successful formation of GOF.

3.2. Effective factors on the adsorption of Cd^{+2} and Pb^{+2} using GOF

3.2.1. Effect of pH

The solution has a pH value, which is an essential factor in the adsorbing method through protonation and deprotonation of the functional groups on the surface of the adsorbent. Hence, first, it was attempted to optimize this factor for each of the two analyte ions. To do so, several batch equilibrium experiments were performed to survey the impact of pH in adsorbing Cd^{+2} and Pb^{+2} by GOF adsorbent. The uptake plot of the metal ions onto the GOF adsorbent has been shown in Figure 6. The adsorption of two analytes on GOF adsorbent was found to be remarkably affected by the pH of the solution. The GOF surface consists of numerous active sites and is likely to be positively charged at low pH value levels. The minimum removal of two ions was at pH=3. It could cause a competitive trend in adsorbing between Cd^{+2}, Pb^{+2}, and H^+ in the process of protonation of nano-adsorbent active sites. In the meantime, the groups of carboxyl, hydroxyl, and N atoms of the GOF will be protonated as active sites. This leads to electrostatic repulsive force between the protonated groups and the metal cations, which, as a result, hinders metal ions from uptake. As the pH increased, the H^+ charges in the solution decreased, and the adsorption percentage increased with increasing pH due to the diminishing of H^+. Strong electrostatic interaction occurs between adsorbent active sites and metal ions, especially the

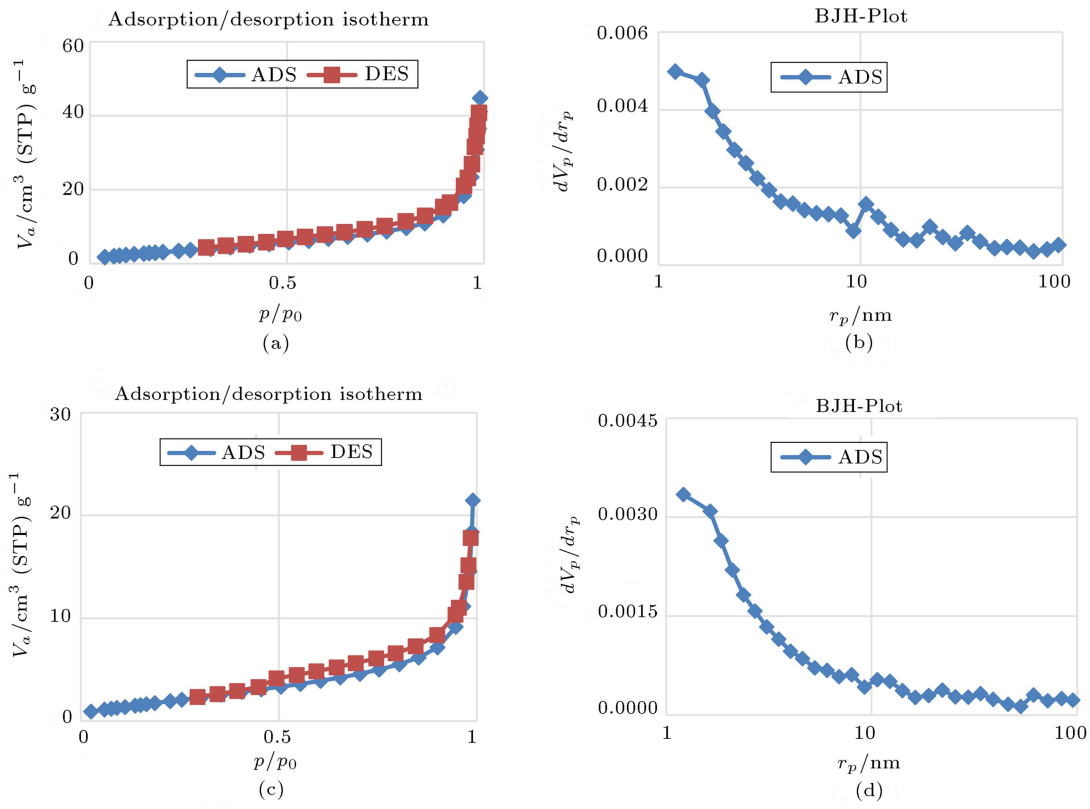

Figure 5. Nitrogen adsorption-desorption isotherm (a) and (c) of GOF and GO, respectively, and pore size distribution (b) and (d) of GOF and GO, respectively.

Table 2. Specific surface area (S_{BET}), diameter pore, and total pore volume of GO and GOF.

Sample	BET surface area (m^2 g^{-1})	Diameter pore (nm)	Total pore volume (cm^3 g^{-1})
GO	7.87	16.70	0.03
GOF	14	19	0.07

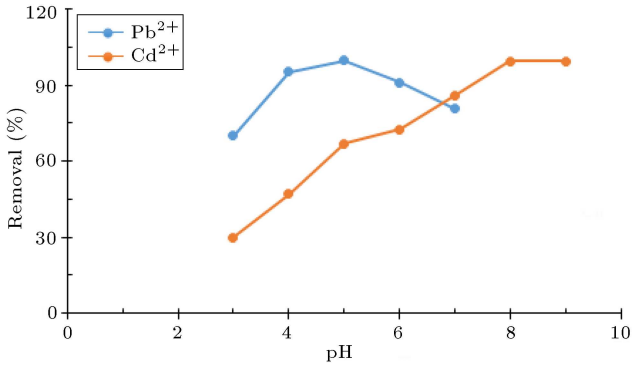

Figure 6. The result of pH on the removal of 10 mg L^{-1} of Cd^{+2} and Pb^{+2} by GOF (Condition: adsorbent dosage, 0.01 g; ultrasonic time, 2 min; the volume of solution, 15 mL).

nitrogen atoms of amino groups and triazine on the adsorbent surface. Besides, when the pH increases, protonation active sites are diminished, and the surface of GOF will have more free nitrogen and oxygen with lone pairs of electrons to coordinate with the ions of Cd^{2+} and Pb^{+2}. The maximum removal is observed at pH=8 for Cd^{+2} and pH=5 for Pb^{+2}.

3.2.2. Adsorbent dosage

The impact of the adsorbent dosage on the efficiency of removing Cd^{+2} and Pb^{+2} was examined to evaluate the optimum amount of GOF (Figure 7). The result showed that by increasing the mass of the adsorbent from 5 to 10 mg, the removal efficiency was increased due to an increase in the number of active sites. But, by increasing the adsorbent amount to 15 mg, no more increment was observed, and the removal efficiency was almost constant. Thus, at higher adsorbent quantities, no notable differences were observed in the trend of the removal efficiency. Because the concentration of metal ions became fixed (equilibrium mode). Accordingly, the adsorbent dosage of 10 mg was chosen for both metal ions as an optimum amount of the adsorbent.

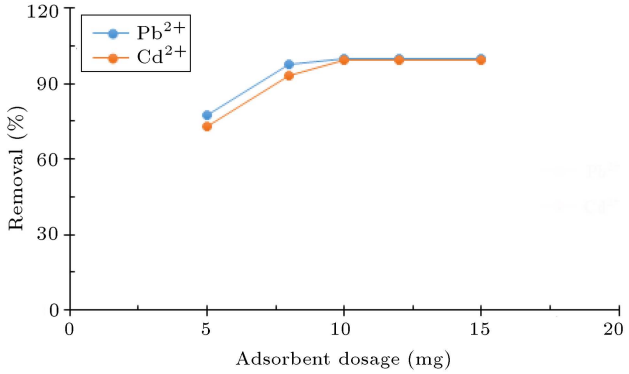

Figure 7. The result of adsorbent dosage on the removal of 10 mg L^{-1} of Cd^{+2} and Pb^{+2} by GOF (Condition: pH=8 for Cd^{+2} and pH=5 for Pb^{+2}; ultrasonic time, 2 min; the volume of solution, 15 mL).

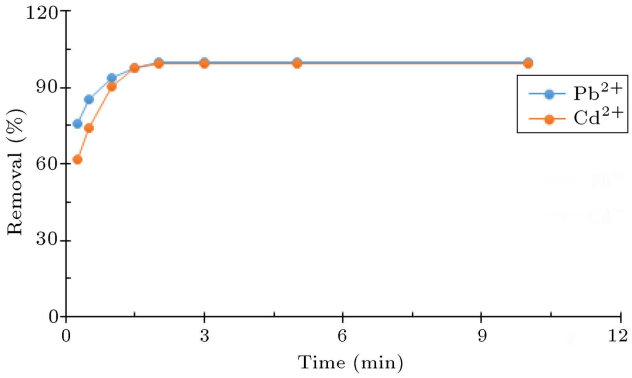

Figure 8. The result of contact time on the removal of 10 mg L^{-1} of Pb^{+2} and Cd^{+2} by GOF (Condition: adsorbent dosage, 0.01 g; pH=5 for Pb^{+2} and pH=8 for Cd^{+2}; the volume of solution, 15 mL).

3.2.3. Contact time

Some tests had to be done to determine the optimal contact time for the adsorption of heavy metal ions by the GOF adsorbent. To do so, the removal capacity of separate analyte ions was examined as a time function. The impact of ultrasonic duration on the adsorbing analytes in the scope of 0.25–10 min was studied. Figure 8 presents the adsorption curves of GOF for Pb^{+2} and Cd^{+2} for various time intervals. Notably, the uptake of Pb^{+2} and Cd^{+2} by GOF adsorbent requires only 2 min to reach the maximum removal efficiency, and the adsorption rate considerably was higher than that of conventional adsorbents [37,38]. The maximum removal rate was observed within 2 min after the start point. After that, the removal of analytes remains almost constant at higher contact times. These results show that 2 min was considered for the equilibrium time. More than 98% of both analytes were removed from the solution at equilibrium status.

3.2.4. Initial Pb^{+2} and Cd^{+2} concentration

To investigate the impact of the initial Pb^{+2} and Cd^{+2} concentration on the removal percentage and

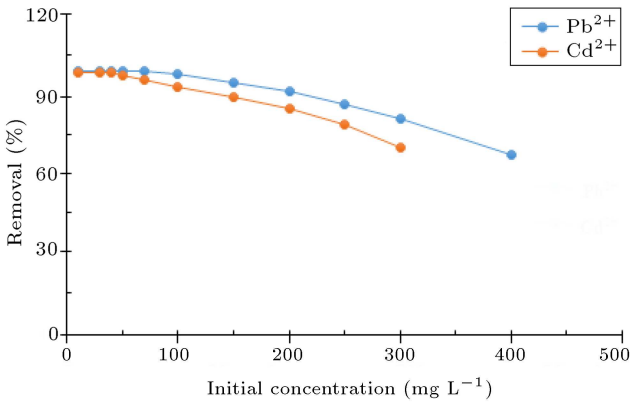

Figure 9. The result of the initial concentration of Cd^{+2} and Pb^{+2} on their removal using GOF (Condition: ultrasonic time, 2 min; adsorbent dosage, 0.01 g; pH=8 for Cd^{+2} and pH=5 for Pb^{+2}; the volume of solution, 15 mL).

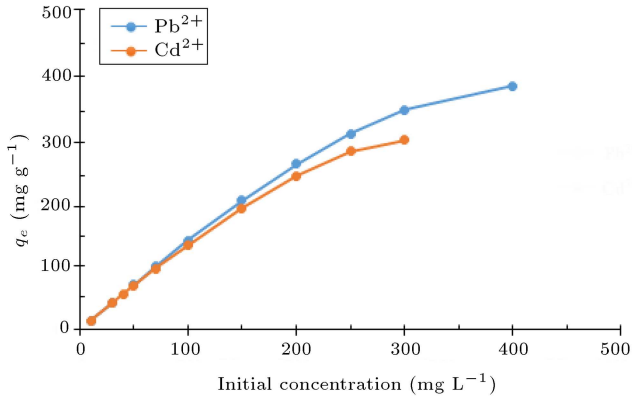

Figure 10. The result of initial metal ion concentration on the adsorption capacities of Cd^{+2} and Pb^{+2} using GOF. (Condition: ultrasonic time, 2 min; adsorbent dosage, 0.01 g; pH=8 for Cd^{+2} and pH=5 for Pb^{+2}; volume of solution, 15 mL).

adsorption capacities by adsorbent (GOF), several experiments were performed with various initial concentrations, in the range of 10–400 mg L^{-1} for Pb^{+2} and 10–300 mg L^{-1} for Cd^{+2}. There was an increment in the adsorption capacity of analyte metal ions and a reduction in the removal percentage by increasing initial concentrations of target ions due to the lack of available active sites for the content of analytes (Figures 9 and 10) [39]. It is widely known that higher initial concentration contributes to enhancing mass transfer power from the solution to the adsorbent surface [40]. This can explain why the driving force for the mass transfer of analytes is great at their high initial concentrations. It showed that increasing initial concentrations of heavy metal ions affected the driving force at the solid-liquid interface, which increased the adsorption capacity until the adsorption sites were saturated. So, using heavy metal ions with an excessive initial concentration caused a decrease in adsorption efficiency for the later adsorption stage [41].

3.3. The isotherm of adsorption

The models of Langmuir and Freundlich isotherms are mathematical and analytical patterns. These models describe the concentration and dispersion of the aqueous and pollution phases at an equilibrium status with the phases of adsorbent and solution. Furthermore, these models for adsorption isotherm have a vital role in determining the sorption behavior. The Langmuir equation is represented in Eq. (3). It displays monolayer adsorption on a homogenous surface where the adsorbing process can solely befall in localized active sites. Usually, for multilayer adsorbing at the heterogeneous surfaces, the Freundlich Eq. (4) is employed:

$$\frac{C_e}{q_e} = \frac{1}{q_{\max} K_1} + \frac{C_e}{q_{\max}}, \tag{3}$$

$$Lnq_e = LnK_f + \frac{1}{nLnC_e}. \tag{4}$$

In this state, the constants of Langmuir and Freundlich are K_1 (L mg^{-1}) and K_f (L mg^{-1}), which are approximately calculated from the plot between C_e/q_e and C_e and between Lnq_e and LnC_e, respectively. The q_e is the equilibrium adsorption capacity (mg g^{-1}), the C_e is the equilibrium concentration (mg L^{-1}), and the q_m is the maximum capacity for adsorbing metal ions (mg g^{-1}). The adsorption isotherms indicate the communication of the equilibrium concentration of the analytes and the adsorbed quantity. Furthermore, it helps to develop effective adsorption systems by presenting valuable data about the probable adsorption mechanisms. In this research, the experimental data related to adsorbing ions of Cd^{+2} and Pb^{+2} for GOF adsorbent were compatible with the adsorption equations of Langmuir and Freundlich to calculate various adsorption parameters (Figures 11 and 12). Considering related data presented in Table 3, it was found that the Langmuir equation (for both Cd^{+2} and Pb^{+2}) with $R^2 > 0.990$ well met the isotherm data. The fitness of Langmuir data to interpret experiments suggested that the adsorptions of Cd^{+2} and Pb^{+2} were restricted

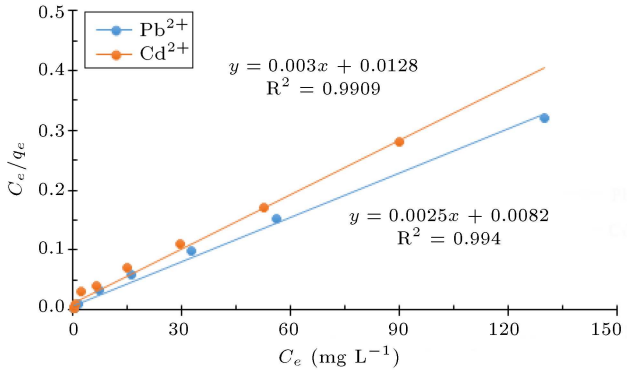

Figure 11. The Langmuir isotherms for the adsorption of Cd^{+2} and Pb^{+2} on GOF adsorbent.

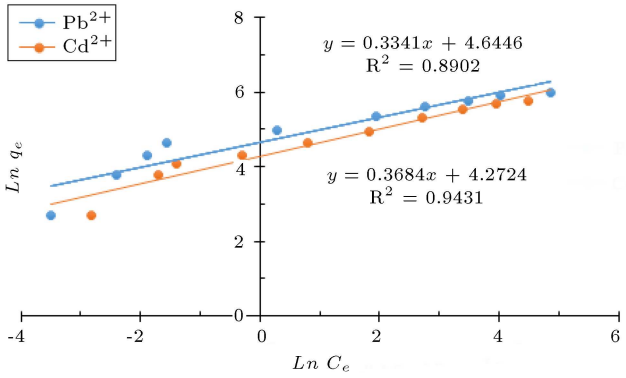

Figure 12. The Freundlich isotherms for the adsorption of Cd^{+2} and Pb^{+2} on GOF adsorbent.

Table 3. Isotherm parameters for the adsorption of Cd^{+2} and Pb^{+2} using GOF.

Model		Parameters	Pb^{+2}	Cd^{+2}
Isotherm	Langmuir	q_m (mg g^{-1})	400	333.33
		K_1 (L mg^{-1})	0.30	0.23
		R^2	0.99	0.99
	Freundlich	K_f (L mg^{-1})	104.02	71.69
		n	2.99	2.71
		R^2	0.89	0.94

to monolayer cover. Also, considering the functional groups with notable interaction with targeted analyte ions, the surface was almost homogenous.

Based on the data reported in Table 3, it could be found that the q_m of GOF was equal to or rather than the other studied adsorbents. This could be related to the excellent combining desire of active groups such as triazine, carboxylic, amine, and hydroxyl to produce steady complexes with Pb^{+2} and Cd^{+2}.

3.4. Kinetic study

In the adsorption process, kinetics studies play a significant role as they provide vital knowledge about the mechanism and pathway of reaction; they can also describe the uptake rate of solutes from an aqueous environment to a solid-phase interface. Hence, kinetics models were utilized for predicting changes in adsorbed analytes over time by applying synthesized GOF adsorbent. The pseudo-first-order and pseudo-second-order equations were applied to analyze the experimental data. By doing so, it was possible to provide the kinetic models representing adsorbing Cd^{+2} and Pb^{+2} ions on GOF. Table 4 shows the related rate equations.

In these two equations, q_e (mg g^{-1}) and q_t (mg g^{-1}) were adsorption capacity at equilibrium and the time (min), respectively. Also, the k_1 (min^{-1}) was the rate constant of the pseudo-first-order, and the k_2 (g mg^{-1} min^{-1}) was the rate constant of the pseudo-

Table 4. Parameters and kinetics models for the adsorption of Cd^{+2} and Pb^{+2} using GOF.

Model	Parameters	Pb^{+2}	Cd^{+2}
Pseudo-firs order: $Ln\ (q_e - q_t) = Ln\ q_e - k_1 t$	k_1 (min)	2.038	2.510
	$q_{e(cal)}$ (mg g^{-1})	6.097	12.480
	R^2	0.990	0.980
Pseudo-second-order: $\frac{t}{q_t} = \frac{1}{k_2 q_e^2} - \frac{t}{q_e}$	k_2 (g mg^{-1} min^{-1})	0.590	0.270
	$q_{e(cal)}$ (mg g^{-1})	15.720	16.640
	R^2	0.999	0.999
Experimental data	$q_{e(exp)}$	14.950	14.910

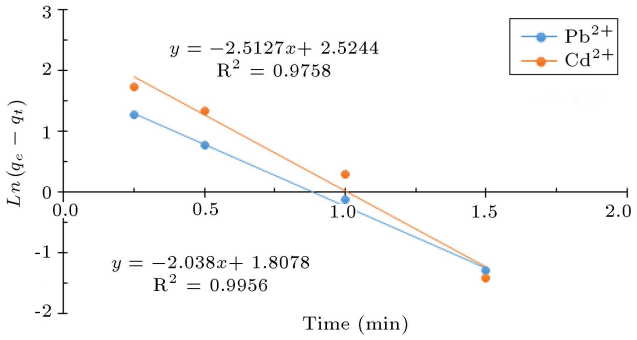

Figure 13. Pseudo-first-order kinetics models for the adsorption of Cd^{+2} and Pb^{+2} on GOF.

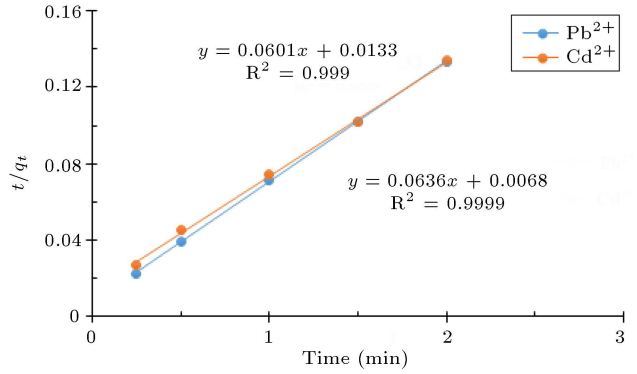

Figure 14. Pseudo-second order kinetics models for the adsorption of Cd^{+2} and Pb^{+2} on GOF.

second-order. All values of the kinetic parameters were computed by plotting the $Ln\ (q_e - q_t)$ and t/q_t versus t associated with the pseudo-first-order and pseudo-second-order model, respectively. Results in Figures 13 and 14 clearly show that the theoretical q_e values calculated by the pseudo-second-order model for both Cd^{+2} and Pb^{+2} ions were almost near the experimental q_{exp} values than the other model. Since R^2 amounts were more than 0.990, adsorbing Pb^{+2} and Cd^{+2} by GOF was properly illustrated by the kinetic model of pseudo-second-order. This demonstrated that the source of the mighty chemical energy between the adsorbent and the adsorbates was the mighty surface complexation of metal ions with the GOF functional groups [42,43].

3.5. Adsorption mechanism

The process by which metal ions are adsorbed via graphene oxide might be associated with surface complexation, ion exchange, and electrostatic with epoxide, hydroxyl, and carboxyl groups based on pH [44,45]. However, because of the restrictions of the functional groups and improperly interacting with the ions of heavy metals, GOF was prepared with H3TATAB, a robust complexing agent, which contained triazine and the amino group. Using this linker in the structure of GOF improved adsorption properties. The linked H3TATAB on the GO sheets as a robust bidentate ligand developed special linkage potential toward ions of most heavy metals and formed complexes with targeted ions by chelation. Typically, GO has epoxide, hydroxyl, and carboxyl groups, but they do not have powerful linking sites like H3TATAB. At pH=8 for Cd^{+2} and pH=5 for Pb^{+2} as optimum pH, the functional groups of H3TATA and other groups containing oxygen are present on the GOF surface in the deprotonated and ionized forms. In such a situation, the process of adsorbing metal ions was under the domination of a powerful surface complexation with H3TATAB and the interactions of electrostatic forces with groups containing oxygen. It was found that the order of GOF capacity for adsorption of both heavy metal ions tested was Pb^{+2}>Cd^{+2}. These differing amounts may be caused by various complexation mechanisms and the metal ions, tendency toward a number of functional groups [46–49].

3.6. Effect of interference ions

The presence of foreign ions in the solution can have a remarkable effect on the adsorption of target ions on the surface of the adsorbent. To examine the reliability of the proposed method, different foreign ions (Zn^{+2}, Ni^{+2}, Fe^{+2}, NO_3^{-1}, and Cl^{-1}) were added to a 25 mL standard solution containing 10 mg mL^{-1} Cd^{+2} and Pb^{+2} ions, and the removal procedure was performed

according to the general procedure. The tolerable limit was defined as the highest number of foreign ions that produced an error not exceeding 5% in the removal of Cd^{+2} and Pb^{+2} ions. The results showed that the extraction by the synthesized absorbent does not affect the presence of these ions and indicates the selectivity of the adsorbent toward the target ion. Additionally, adsorbents can be used in samples that typically have this ion in a high percentage.

3.7. Analysis of the real sample

Due to the heterogeneity and complicacy of real samples, the removal efficiency of adsorbent on the model wastewater prepared in the laboratory might be different from that of the environmental water samples. So, it is necessary to investigate the efficiency of adsorbent under real environmental samples. The removal procedure by synthesized adsorbents was successfully applied to remove Cd^{+2} and Pb^{+2} ions spiked to different water samples (Karoon river). The results showed that under the optimized conditions, more than 95% (RSD<3%) of the Cd^{+2} and Pb^{+2} ions could be removed from the aqueous solution. As a result, this adsorbent is feasible and suitable for application at the field level.

3.8. Comparing this adsorbent and technique with some different adsorbents

The extraction efficiency of the presented method was compared with other reported methods from the viewpoint of adsorbent capacity and time of extraction [10,49-53]. Comparison results of the remarkable efficiency of GOF adsorbent and proposed method with different existing methods for adsorption and removal of Cd^{+2} and Pb^{+2} is exhibited in Table 5. The selection of the most suitable adsorbent depends on several items, including cost-effectiveness, extraction efficiency, extraction time, and reusability. However, most of these techniques have several limitations, such as much time to analyze and low capacity. These limitations make them unsuitable for conventional analysis of cases. These results show that the new synthesized GOF has high extraction efficiency and a very short extraction time. This can be due to the differences in adsorbent properties such as chemical structure, surface area, porosity, and functional groups. According to the results, it is clear that the chosen ligand and technique to fabricate GOF and find optimal conditions with the help of the ultrasonic approach were sufficient for the best performance of the GOF adsorbent.

3.9. Reusability of adsorbent

The regeneration and reuse of adsorbents are one of the most important challenges in assessing their potential for practical applications. After regenerating the GOF adsorbent, it would be reusable to uptake the analytes of Pb^{+2} and Cd^{+2}. After every extracting process, the adsorbent simply underwent regeneration by washing with 10 mL of HCl 0.2 M to make it reusable. It was found that the GOF adsorbent was reusable five times, and it preserved the capacity to absorb at a relatively steady value (Figure 15). By assessing the adsorbent constancy over several months, it was determined that it was steady for at least 12 months. Finally, the GOF, with excellent abilities for adsorption and outstanding

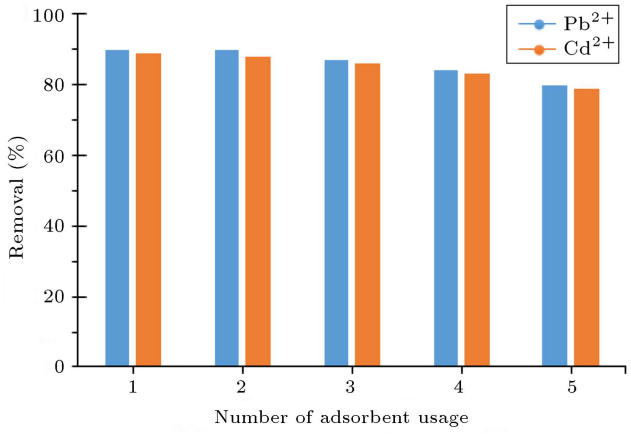

Figure 15. Reusability of the GOF adsorbent for the adsorption of Cd^{+2} and Pb^{+2} ions.

Table 5. Evaluation of adsorption capacities of various adsorbents for Cd^{+2} and Pb^{+2}.

Entry	Adsorbent	Adsorption capacity (mg g^{-1})		Contact time (min)	Ref.
		Pb^{+2}	Cd^{+2}		
1	Zeolite N.P./PEG/GO	49.6	50.2	20	[49]
2	rGO-Fe_3O_4@polydopamine	35.2	–	–	[10]
3	Oak wood ash/GO/Fe_3O_4	47.16	43.66	–	[50]
4	Cyclodextrin-GO	–	222.2	120	[51]
5	Zeolitic imidazolate framework-L/GO	27.7	172.4	–	[52]
6	Magnetic iron oxide/GO	–	52.1	180	[53]
7	GOF	400.0	333.3	2	This work

capability to be recycled in all respects, is a perfect adsorbent to remove ions of heavy metals.

4. Conclusion

In this paper, a new Graphene Oxide Framework (GOF) has been successfully synthesized and characterized. The GOF exhibits superior adsorption performance for contaminants of Pb^{+2} and Cd^{+2}. According to integrating the in-depth bulk adsorption and the surface adsorption, scholars attribute this property to the interlinked pore network of GOF and the impact of interlayer trapping. Some factors influencing the amounts of adsorbing Pb^{+2} and Cd^{+2} were examined, including the adsorbent amount, the ions, primary concentration, solution pH, and contact duration. The results of batch adsorption were properly matched with the Langmuir model with the q_m of 333.3 m^2/g for Cd^{+2} and 400.0 m^2/g for Pb^{+2}. These results were notably better in comparison to graphene oxide. The sorption mechanism included chelating the electrostatic interaction between GOF nano-sorbent, Cd^{+2} and Pb^{+2} and interaction $\pi-\pi$ stacking. The GOF-specific characteristics (high adsorption amount, high removal efficiency, and excellent recyclability), together with the stability, make the shown heterogeneous system very desirable from the green chemistry point of view. Finally, these encouraging results indicate that the suggested technique involving the chosen linker, the technique to modify GO, and finding the optimal conditions accelerated by ultrasonic was adequate for the GOF adsorbent to have the best performance.

Acknowledgment

We acknowledge Shahid Chamran University of Ahvaz Research Council, Ahvaz, for financial support of this investigation (grant number: SCU.SC99.232).

References

1. Shegefti, S., Mehdinia, A., and Shemirani, F. "Preconcentration of cobalt(II) using polythionine-coated Fe_3O_4 nanocomposite prior its determination by AAS", *Microchimica Acta*, **183**, pp. 1963–1970 (2016).
2. Leung, W.C., Wong, M.F., Chua, H., et al. "Removal and recovery of heavy metals by bacteria isolated from activated sludge treating industrial effluents and municipal wastewater", *Water Science and Technology*, **41**, pp. 233–240 (2000).
3. Ricco, R., Konstas, K., Styles, M.J., et al. "Lead (II) uptake by aluminium based Magnetic Framework Composites (MFCs) in water", *Journal of Materials Chemistry*, A., **3**, pp. 19822–19831 (2015).
4. Crittenden, J.C., Howe, K.J., Hand, D.W., et al., *Principles of Water Treatment*, John Wiley and Sons, Incorporated (2012).
5. Bodagh, A., Khoshdast, H., Sharafi, H., et al. "Removal of cadmium(II) from aqueous solution by ion flotation using rhamnolipid biosurfactant as an ion collector", *Industrial and Engineering Chemistry Research*, **52**, pp. 3910–3917 (2013).
6. Wu, Y., Luo, H., Wang, H., et al. "Adsorption of hexavalent chromium from aqueous solutions by graphene modified with cetyltrimethyl ammonium bromide", *Journal of Colloid and Interface Science*, **394**, pp. 183–191 (2013).
7. (a) Kim, D.G. and Ko, S.O. "A dual media filter using zeolite and mortar for the efficient removal of heavy metals in stormwater runoff", *Water*, **14**, p. 3567 (2022); (b) Liu, Y., Xue, F., Wang, T., et al. "Three-dimensional ordered zeolite-templated carbon with covalent sulfur for efficient removal of elemental mercury: Experimental study and molecular dynamic simulation", *Fuel Processing Technology*, **239**, p. 107540 (2023).
8. Yadav, V.B., Gadi, R., and Kalra, S. "Clay based nanocomposites for removal of heavy metals from water: A review", *Journal of Environmental Management*, **232**, pp. 803–817 (2019).
9. Zhang. T., Wang, W., Zhao, Y., et al. "Removal of heavy metals and dyes by clay-based adsorbents: From natural clays to 1D and 2D nano-composites", *Chemical Engineering Journal*, **420**, p. 127574 (2021).
10. Mehdinia, A., Heydari, S., and Jabbari, A. "Synthesis and characterization of reduced graphene oxide-Fe_3O_4@polydopamine and application for adsorption of leadions: Isothermandkineticstudies", *Materials Chemistry and Physics*, **239**, pp. 121964–121974 (2020).
11. Tang, P., Sun, Q., Zhao, L., et al. "A simple and green method to construct cyclodextrin polymer for the effective and simultaneous estrogen pollutant and metal removal", *Chemical Engineering Journal*, **366**, pp. 598–607 (2019).
12. Kobielska, P.A., Howarth, A.J., Farha, O.K., et al. "Metal-organic frameworks for heavy metal removal from water", *Coordination Chemistry Reviews*, **358**, pp. 92–107 (2018).
13. Xu, G.R., An, Z.H., Xu, K., et al. "Metal Organic Framework (MOF)-based micro/nanoscaled materials for heavy metal ions removal: The cutting-edge study on designs, synthesis, and applications", *Coordination Chemistry Reviews*, **427**, 213554 (2021).
14. Gendy, E.A., Ifthikar, J., Ali, J., et al. "Removal of heavy metals by Covalent Organic Frameworks (COFs): A review on its mechanism and adsorption properties", *Journal of Environmental Chemical Engineering*, **9**, 105687 (2021).
15. Zhong, X., Liu, Y., Liang, W., et al. "Construction of core-shell MOFs@COF hybrids as a platform for the removal of UO_2^{2+} and Eu^{3+} ions from solution", *ACS Applied Materials Interfaces*, **13**, pp. 13883–13895 (2021).

16. Klionsky, D.J., Abdalla, F.C., Abeliovich, H., et al. "Guidelines for the use and interpretation of assays for monitoring autophagy", *Autophagy*, **8**, pp. 445–544 (2012).

17. Merceille, A., Weinzaepfel, E., Barre, Y., and Grandjean, A. "The sorption behaviour of synthetic sodium nonatitanate and zeolite A for removing radioactive strontium from aqueous wastes", *Separation and Purification Technology*, **96**, pp. 81–88 (2012).

18. Arshad, F., Selvaraj, M., Zain, J., et al. "Polyethylenimine modified graphene oxide hydrogel composite as an efficient adsorbent for heavy metal ions", *Separation and Purification Technology*, **209**, pp. 870–880 (2019).

19. Gabris, M.A., Jume, B.H., Rezaali, M., et al. "Novel magnetic graphene oxide functionalized cyanopropyl nanocomposite as an adsorbent for the removal of Pb(II) ions from aqueous media: equilibrium and kinetic studies", *Environmental Science and Pollution Research*, **25**, pp. 27122–27132 (2018).

20. Ma, Y.X., Kou, Y.L., Xing, D., et al. "Synthesis of magnetic graphene oxide grafted polymaleicamide dendrimer nanohybrids for adsorption of Pb(II) in aqueous solution", *Journal of Hazardous Materials*, **340**, pp. 407–416 (2017).

21. Peer, F.E., Bahramifar, N., and Younesi, H. "Removal of Cd(II), Pb(II) and Cu(II) ions from aqueous solution by polyamidoamine dendrimer grafted magnetic graphene oxide nanosheets", *Journal of the Taiwan Institute of Chemical Engineers*, **87**, pp. 225–240 (2018).

22. Wang, X., Liu, Y., Pang, H., et al. "Effect of graphene oxide surface modification on the elimination of Co(II) from aqueous solutions", *Chemical Engineering Journal*, **344**, pp. 380–390 (2018).

23. Zare-dorabei, R., Moazen, S., Barzin, A., et al. "Highly efficient simultaneous ultrasonic-assisted adsorption of Pb(II), Cd(II), Ni(II) and Cu(II) ions from aqueous solutions by graphene oxide modified with 2,2'-dipyridylamin: central composite design optimization", *Ultrasonics Sonochemistry*, **32**, pp. 265–276 (2016).

24. Yin, N., Wang, K., Xia, Y.A., et al. "Novel melamine modified metal-organic frameworks for remarkably high removal of heavy metal Pb(II)", *Desalination*, **430**, pp. 120–127 (2018).

25. Tan, M.X., Sum, Y.N., Ying, J.Y., et al. "A mesoporous poly-melamine-formaldehyde polymer as a solid sorbent for toxic metal removal", *Energy and Environmental Science*, **6**, pp. 3254–3259 (2013).

26. Wang, X., Li, R., Liu, J., et al. "Melamine modified graphene hydrogels for the removal of uranium(VI) from aqueous solution", *New Journal of Chemistry*, **41**, pp. 10899–10907 (2017).

27. Li, K., Wu, G., Wang, M., et al. "Efficient removal of lead ions from water by a low-cost alginate-melamine hybrid sorbent", *Applied Sciences*, **8**, pp. 1518–1530 (2018).

28. Hummers, W.S. and Offemann, R.E. "Preparation of graphitic oxide", *Journal of the American Chemical Society*, **80**, p. 1339 (1958).

29. Fang, Q.R., Yuan, D.Q., Sculley, J., et al. "Functional mesoporous metal-organic frameworks for the capture of heavy metal ions and size-selective catalysis", *Inorganic Chemistry*, **49**, pp. 11637–11642 (2010).

30. Shekarizadeh, A. and Azadi, R. "Synthesis of Pd@graphene oxide framework nanocatalyst with enhanced activity in Heck-Mizoroki cross-coupling reaction", *Applied Organometallic Chemistry*, **e5775**, pp. 1–8 (2020).

31. Liu, J., Ge, X., Ye, X., et al. "3D graphene/δ-MnO_2 aerogels for highly efficient and reversible removal of heavy metal ions", *Journal of Materials Chemistry*, A., **4**, pp. 1970–1979 (2016).

32. Yu, B., Wang, X., Xing, W.Y., et al. "UV-curable functionalized graphene oxide/polyurethane acrylate nanocomposite coatings with enhanced thermal stability and mechanical properties", *Industrial and Engineering Chemistry Research*, **51**, pp. 14629–14636 (2012).

33. Hu, W., Zhan, J., Wang, X., et al. "Effect of functionalized graphene oxide with hyper-branched flame retardant on flammability and thermal stability of cross-linked polyethylene", *Industrial and Engineering Chemistry Research*, **53**, pp. 3073–3083 (2014).

34. Zare, E.N., Lakouraj, M.M., and Kasirian, N. "Development of effective nano-bio sorbent based on poly m-phenylenediamine grafted dextrin for removal of Pb (II) and methylene blue from water", *Carbohydrate Polymers*, **201**, pp. 539–548 (2018).

35. Santhosh, C., Nivetha, R., Kollu, P., et al. "Removal of cationic and anionic heavy metals from water by 1D and 2D-carbon structures decorated with magnetic nanoparticles", *Scientific Reports*, **7**, pp. 14107–14118 (2017).

36. Guo, X., Du, B., Wei, Q., et al. "Synthesis of amino functionalized magnetic graphene composite material and its application to remove Cr(VI), Pb(II), Hg(II), Cd(II) and Ni(II) from contaminated water", *Journal of Hazardous Materials*, **278**, pp. 211–220 (2014).

37. Kadirvelu, K., Faur-Brasquet, C., and Cloirec, P.L. "Removal of Cu(II), Pb(II), and Ni(II) by adsorption onto activated carbon cloths", *Langmuir*, **16**, pp. 8404–8409 (2000).

38. Samuel, M.S., Sheriff, S., Bhattacharya, J., et al. "Adsorption of Pb(II) from aqueous solution using a magnetic chitosan/graphene oxide composite and its toxicity studies", *International Journal of Biological Macromolecules*, **115**, pp. 1142–1150 (2018).

39. Eren, Z. and Acar, F.N. "Adsorption of reactive black 5 from an aqueous solution: equilibrium and kinetic studies", *Desalination*, **194**, pp. 1–10 (2006).

40. Hayati, B., Maleki, A., Najafi, F., et al. "Super high removal capacities of heavy metals (Pb(2+) and Cu(2+)) using CNT dendrimer", *Journal of Hazardous Materials*, **336**, pp. 146–157 (2017).

41. Mohan, S., Kumar, V., Singh, D.K., et al. "Effective removal of lead ions using graphene oxide-MgO nanohybrid from aqueous solution: isotherm, kinetic and thermodynamic modeling of adsorption", *Journal of Environmental Chemical Engineering*, **5**, pp. 2259–2273 (2017).

42. Sitko, R., Turek, E., Zawisza, B., et al. "Adsorption of divalent metal ions from aqueous solutions using graphene oxide", *Dalton Transactions*, **42**, pp. 5682–5689 (2013).

43. Cheng, C., Liu, Z., Li, X., et al. "Graphene oxide interpenetrated polymeric composite hydrogels as highly effective adsorbents for water treatment", *RSC Advanced*, **4**, pp. 42346–42357 (2014).

44. Ghaedi, M., Hajati, S., Zare, M., et al. "Experimental design for simultaneous analysis of malachite green and methylene blue; derivative spectrophotometry and principal component-artificial neural network", *RSC Advanced*, **5**, pp. 38939–38947 (2015).

45. Wu, W., Yang, Y., Zhou, H., et al. "Highly efficient removal of Cu(II) from aqueous solution by using graphene oxide", *Water, Air, and Soil Pollution*, **224**, pp. 1–8 (2013).

46. Luo, S., Xu, X., Zhou, G., et al. "Amino siloxane oligomer-linked graphene oxide as an efficient adsorbent for removal of Pb(II) from wastewater", *Journal of Hazardous Materials*, **274**, pp. 145–155 (2014).

47. Lei, Y., Chen, F., Luo, Y., et al. "Synthesis of three-dimensional graphene oxide foam for the removal of heavy metal ions", *Chemical Physics Letters*, **593**, pp. 122–127 (2014).

48. Chandra, V., Park, J., Chun, Y., et al. "Water-dispersible magnetite-reduced graphene oxide composites for arsenic removal", *ACS Nano*, **4**, pp. 3979–3986 (2010).

49. Samadi, S., Mirzaie-Shalmani, M., and Zakaria, S.A. "Removal of heavy metals from Tehran south agricultural water by Zeolite N.P./PEG/GO nanocomposite", *Journal of Water Environmental Nanotechnology*, **4**, pp. 157–166 (2019).

50. Pelalaki, R., Heidari, Z., Khatami, S.M., et al. "Oak wood ash/GO/Fe_3O_4 adsorption efficiencies for cadmium and lead removal from aqueous solution: Kinetics, equilibrium and thermodynamic evaluation", *Arabian Journal of Chemistry*, **14**, 102991 (2021).

51. Einafshar, E., Khodadaipoor, Z., Nejabat, M., et al. "Synthesis, characterization and application of cyclodextrin-conjugated graphene oxide for removing Cadmium ions from aqueous media", *Journal of Polymers and the Environment*, **29**, pp. 3161–3173 (2021).

52. Ahmad, S.Z.N., Salleh, W.N.W., Ismail, N.H., et al. "Effects of operating parameters on cadmium removal for wastewater treatment using zeolitic imidazolate framework-L/graphene oxide composite", *Journal of Environmental Chemical Engineering*, **9**, 106139 (2021).

53. Thy, L.T.M., Thuong, N.H., Tu, T.H., et al. "Synthesis of magnetic iron oxide/graphene oxide nanocomposites for removal of cadmium ions from water", *Advance in Natural Sciences: Nanoscience and Nanotechnology*, **10**, pp. 025006–025013 (2019).

Biographies

Arezoo Shekarizadeh was born in 1980 in Dezful, Khuzestan, Iran, and developed a keen interest in chemistry at a young age. She pursued higher education in this field, obtaining a BSc degree of Science in Pure Chemistry from Shahid Chamran University of Ahvaz. She then completed her MSc degree in Organic Chemistry at the same university. After completing her MSc degree, she continued her academic pursuits and pursued a PhD degree in Organic Chemistry at Shahid Chamran University of Ahvaz, Faculty of Science, Chemistry Department. In 2021, she successfully graduated with her PhD. Throughout her academic career, she has focused her research interests on organic synthesis and nano-chemistry.

Roya Azadi, was born in 1980 in Shiraz, Iran. She completed her BSc degree of Science in Pure Chemistry from Shiraz University in 2002. After completing her undergraduate studies, she went on to pursue a MSc degree in Organic Chemistry from the same university, which she completed in 2004. In 2008, she received her PhD degree in Organic Chemistry from Shiraz University. Following the completion of her doctoral studies, she joined the faculty at Shahid Chamran University of Ahvaz as a faculty member in the Chemistry Department. Since then, she has been actively engaged in teaching and research activities at the university. She has been recognized for her contributions to the field of Organic Chemistry and has been promoted to the rank of Associate Professor. Her research interests focus on synthesizing and characterizing organic compounds and nanocomposite-based graphene and development applications. Her research has been published in numerous scientific journals, and she has presented her research at various national and international conferences. In addition to her academic work, she is involved in multiple community service activities. She is committed to promoting education and scientific literacy among young people in her community.

Roya Mirzajani was born in 1973 and grew up in Andimeshk, Khuzestan, Iran. She pursued her higher education in Chemistry, earning a BSc degree in Pure Chemistry from Lorestan University. She then went on to complete her MSc degree in Analytical Chemistry at Shiraz University, followed by a PhD degree in the same field at the same university. After completing

her studies, she began her career as a faculty member at Shahid Chamran University of Ahvaz in 2007. She has since risen to the position of Professor and is affiliated with the Analytical Chemistry department of the Chemistry Faculty at the university. She is an active member of the academic community and has published numerous articles in renowned scientific journals. In addition to her academic pursuits, she also mentor and supervise students pursuing their research projects.